

Fermionization in an expanding 1D gas of hard-core bosons

Marcos Rigol and Alejandro Muramatsu
*Institut für Theoretische Physik III, Universität Stuttgart,
 Pfaffenwaldring 57, D-70550 Stuttgart, Germany.*

We show by means of an exact numerical approach that the momentum distribution of a free expanding gas of hard-core bosons on a one-dimensional lattice approaches to the one of noninteracting fermions, acquiring a Fermi edge. Yet there is a power-law decay of the one-particle density matrix $\rho_x \sim 1/\sqrt{x}$, as usual for hard-core bosons in the ground state, which accounts for a large occupation of the lowest natural orbitals for all expansion times. The fermionization of the momentum distribution function, which is not observed in equilibrium, is analyzed in detail.

PACS numbers: 03.75.Kk, 03.75.Lm, 05.30.Jp

At very low temperatures and densities a one-dimensional (1D) gas of bosons is expected to behave as a gas of impenetrable particles known as hard-core bosons (HCB) [1]. Two recent experiments successfully achieved the required parameter regime and made HCB a physical reality [2, 3]. In contrast to bosons in higher dimensions, 1D HCB share many properties with noninteracting spinless fermions to which they can be mapped [4]. Thermodynamic properties like the total energy, and microscopic properties like density profiles are identical in both systems. On the contrary, quantities like the momentum distribution function (n_k) [5] and the so-called natural orbitals (NO) [6] are very different for HCB and spinless fermions. This is due to the different behavior of the off-diagonal elements of the one-particle density matrix (OPDM) in both systems (see *e.g.* Ref. [7]).

An important point for the comparison between experimental results and theory in Refs. [2, 3] has been the awareness of the effects of the trapping potential in the properties of the HCB gas. On a harmonic trap it has been found that the power-law decay of the OPDM $\rho_{ij} \sim |x_i - x_j|^{-1/2}$, known from homogeneous systems [5], is renormalized by a factor that depends on the density at points i and j . This factor is proportional to $[n_i n_j]^{1/4}$ for continuous systems [8], and to $[n_i(1 - n_i)n_j(1 - n_j)]^{1/4}$ for HCB on a lattice [9]. Furthermore, the power-law decay of the OPDM has been found to be universal independently of the power of the confining potential [9]. Even for systems out of equilibrium, that start their evolution from a totally uncorrelated state, the power law above develops dynamically and leads to the emergence of quasi-condensates at finite momentum [10].

In this work we show that during the free expansion of 1D HCB in a lattice a further degree of fermionization takes place, *i.e.*, n_k of the HCB becomes for long expansion times equal to the one of noninteracting fermions, displaying a Fermi edge. This feature, absent in equilibrium, can be easily confirmed experimentally with a setup like the one in Ref. [3] where the expansion of the 1D gas was studied after removing the axial confinement. Other quantities like the OPDM and the NO still evidence the strongly interacting character of the HCB system.

We obtain the exact dynamics of expanding clouds of HCB on 1D lattices on the basis of the Jordan-Wigner transformation, which maps the HCB Hamiltonian into the one of spinless fermions [10]. Apart from being exact, our method allows to consider relatively large number of particles and system sizes, which can be even larger than the ones in the present experimental setups. Results for continuous systems can be extrapolated from very low densities in the lattice [9]. At time $\tau = 0$ we switch off the trapping potential, and start the time evolution from the ground state of the HCB Hamiltonian

$$H_{HCB} = -t \sum_i (b_i^\dagger b_{i+1} + \text{H.c.}) + V_2 \sum_i x_i^2 n_i, \quad (1)$$

which has the additional on-site constraints $b_i^{\dagger 2} = b_i^2 = 0$, $\{b_i, b_i^\dagger\} = 1$. In Eq. (1), b_i^\dagger and b_i represent the HCB creation and annihilation operators, respectively, $n_i = b_i^\dagger b_i$ the particle number operator, t the hopping parameter, and V_2 the curvature of the harmonic confining potential.

In order to characterize the initial state, we use the characteristic density $\tilde{\rho} = N_b a / \zeta$ [9, 10], which for trapped systems plays a similar role than the density in periodic systems. N_b is the number of HCB, $\zeta = (V_2/t)^{-1/2}$ is a length scale of the trap in the presence of the lattice, and a is the lattice constant. The quasi-momentum distribution function n_k is also normalized by the length scale ζ as $n_k = (a/\zeta) \sum_{ij} e^{-ik(i-j)} \rho_{ij}$, with $\rho_{ij} = \langle b_i^\dagger b_j \rangle$. In addition, we define the Fermi momentum k_F associated to the fermions as $\epsilon_F = -2t \cos(k_F a)$, where ϵ_F is the energy of the last occupied fermionic single-particle state in the trap at $\tau = 0$. (Although in the trap n_k is continuous at k_F , it is possible to see that n_k approaches zero even faster than exponentially for $k > k_F$.)

In Fig. 1 we show n_k for an expanding gas of HCB at four different times, and compare it with the one of noninteracting fermions (which does not change during the expansion). Several issues are evident: i) Shortly after switching off the trapping potential, the peak at $n_{k=0}^b$ disappears. ii) For $k < k_F$ a redistribution of the

population of k states takes place, such that starting from $k \sim 0$, n_k of HCB matches in time the one for fermions. iii) k states with $k > k_F$ become less populated and an edge develops at k_F . The overall process leads to an n_k for the HCB that is equal to the one of the fermions.

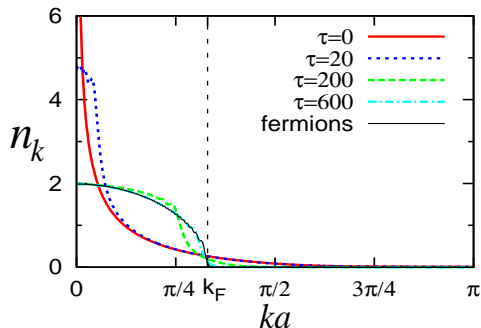


FIG. 1: (color online). n_k for 100 HCB expanding from an initial state with $\tilde{\rho} = 0.51$, compared to the one for the corresponding fermions. Times (τ) are given in units of \hbar/t , and k_F denotes de Fermi momentum as defined in the text.

After observing the fermionization of n_k for HCB, one could naively expect that something similar could be happening with the NO occupations. The NO (ϕ_i^η) are the eigenfunctions of the OPDM $\sum_j \rho_{ij} \phi_j^\eta = \lambda_\eta \phi_i^\eta$ [6], i.e., they are effective single-particle states with occupations λ_η . For noninteracting fermions the NO are the eigenfunctions of the Hamiltonian and their occupation is one. We find that in contrast to n_k the NO occupations do not fermionize, as can be seen in Fig. 2 for the same parameters of Fig. 1.

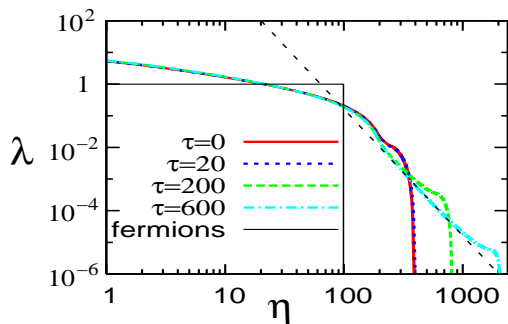


FIG. 2: (color online). Occupation of the NO vs η for the same initial trap parameters and times of Fig. 1. The thin dashed line corresponds to a power law η^{-4} , which is known from equilibrium systems at low densities [9].

There are two features of the NO occupations that we find worth noticing. The first one, which is difficult to distinguish in Fig. 2, is that the lowest natural orbitals slightly increase their occupations during the expansion of the gas. This can be intuitively understood as an increase of the “coherence” of the system due to an increase of the system size, which delocalize the HCB over more lattice sites. Something similar occurs in the ground state

occupations of the lowest natural orbitals when for the same number of particles the curvature of the trap is decreased [9]. However, in equilibrium systems, $n_{k=0}$ also increases with the increase of λ_0 . The apparent contradiction between the decrease of $n_{k=0}$ and the increase of λ_0 in the expanding gas can be resolved observing the Fourier transform of the lowest NO at $\tau = 0$ and $\tau > 0$. As it can be seen in Fig. 3, initially $|\phi_k^0|$ has a peak at $k = 0$ showing that quasi-condensation occurs around $k = 0$, and this is reflected in n_k . For $\tau > 0$ the lowest NO becomes an extended object in k -space so that the HCB forming the quasi-condensate have many different momenta, basically as many as n_k in Fig. 1. Hence, there is no contradiction between the observed behavior of the NO occupations and n_k , although the last one is clearly different to the one of systems in equilibrium.

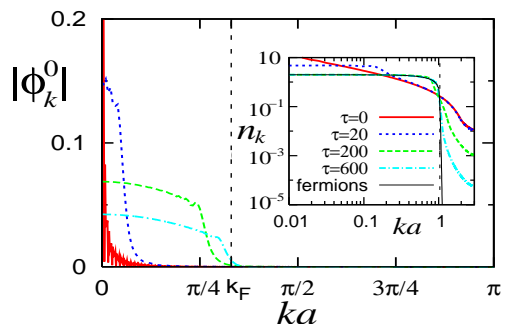


FIG. 3: (color online). Fourier transform of the lowest NO, and n_k in a logarithmic scale (inset), for the same initial trap parameters and times of Figs. 1 and 2. k_F (vertical dashed line) denotes de Fermi momentum.

The second feature that is worth noticing, sets in only when the density of the expanding HCB becomes very low. Then the universal power-law decay of the NO occupations for large- η ($\lambda_\eta \sim A_{N_b} \eta^{-4}$), known from equilibrium systems [9], also appears in nonequilibrium (Fig. 2). In Ref. [9], the prefactor of the power-law A_{N_b} was found to depend only on N_b independently of the confining potential. We find out of equilibrium that A_{N_b} is exactly the same than in the ground state case [9]. For $N_b = 100$ we have plotted $\lambda_\eta = A_{N_b} \eta^{-4}$ in Fig. 2. The long tail of the momentum distribution function $n_k \sim |k|^{-4}$, that in equilibrium appears together with the $\lambda_\eta \sim \eta^{-4}$ [9], is in general not present in nonequilibrium since for large τ , n_k for HCB starts to behave like the one of fermions (inset in Fig. 3).

Considering the previous results for the behavior of the NO occupations, which is similar to the one known in equilibrium [9], one expects that also the OPDM should behave similarly. Since in nonequilibrium $\rho_{ij} = |\rho_{ij}| e^{i\theta_{ij}}$ is in general a complex object, in order to compare with equilibrium systems we first study its modulus. Results for the same systems of Figs. 1–3 are shown in Fig. 4(a). Figure 4(a) shows that $|\rho_{ij}(\tau)|$ have exactly the same form than ρ_{ij} in equilibrium systems [9]. For large values

of $|x_i - x_j|$ a power-law decay $|\rho_{ij}| \sim |x_i - x_j|^{-1/2}$ can be observed *for all times*, and the prefactor of the power law decreases with the reduction of the local densities in the system. Hence, the slow decay of the one-particle correlations is the one accounting for the large ($\sim \sqrt{N_b}$) occupation of the lowest NO. On the other hand, Figs. 4(b)-(d) show that the phase of the OPDM (θ_{ij}) starts

to increasingly oscillate at large distances. In particular Fig. 4(b) shows that after a very short time, when the modulus of the OPDM have almost not changed, θ_{ij} have started to oscillate for $|x_i - x_j| \gg a$ producing a fast destruction of the zero momentum peak in n_k^b , as shown in Fig. 1.

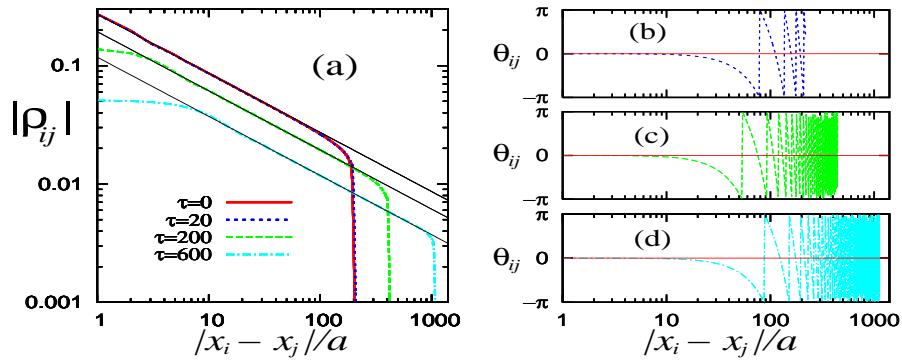


FIG. 4: (color online). Modulus of the OPDM (a) and its phase (b)-(d) for the same initial trap parameters and times of Figs. 1–3. Both quantities have been evaluated with respect to the middle of the expanding cloud of HCB. Thin continuous lines in (a) correspond to power laws $|x_i - x_j|^{-1/2}$.

In order to gain further insight into the fermionization described above, we observe that for noninteracting particles, given the initial one-particle density matrix ρ_{ab} , the density profile at time τ can be evaluated as [11]

$$n_i(\tau) = \sum_{ab} G_{i,a}^*(\tau) G_{i,b}(\tau) \rho_{ab}, \quad (2)$$

where the free one-particle propagator can be written in the form $G_{i,j}(\tau) = \sum_k e^{-i\tau/\hbar[\epsilon_k - \hbar k(x_i - x_j)/\tau]}$, ϵ_k being the dispersion relation. Fourier transforming the initial OPDM into ϱ_{k_1, k_2} and performing straightforward integrations, Eq. (2) can be rewritten as

$$\begin{aligned} n_i(\tau) &= \sum_{k_1, k_2} \varrho_{k_1 k_2} e^{i\tau/\hbar[\epsilon_{k_1} - \hbar k_1 x/\tau]} e^{-i\tau/\hbar[\epsilon_{k_2} - \hbar k_2 x/\tau]} \\ &\simeq \frac{1}{\tau \epsilon''_{k=k_0(x_i/\tau)}} \varrho_{k_1=k_0(x_i/\tau), k_2=k_0(x_i/\tau)}, \end{aligned} \quad (3)$$

where in the last step we have assumed τ to be very large and performed the summations using the saddle point approximation. [$k_0(x_i/\tau)$ is determined by the expression $\epsilon'_{k_0} = \hbar x_i/\tau$, where the prima means k -derivative.] Equation (3) shows that for $\tau \rightarrow \infty$ the density profile is only determined by a rescaling of the diagonal part of ϱ_{k_1, k_2} , which is nothing but n_k . In the continuum limit $\epsilon_k = \hbar^2 k^2/2m$ and $n(x, \tau) \simeq (m/\tau) \tilde{n}(k = mx/\hbar\tau)$ [$\tilde{n}(k)$ is the momentum distribution function], which is a known result that can be also obtained by other means [11]. Since the arguments above are valid for both fermions and bosons, the fact that n_k of HCB converges to that of fermions after expansion could be explained at this

point *if after a certain time, the expanding HCB could be considered as non-interacting*. This would mean that n_k for HCB would be determined by a rescaling of the density profile that, on the other hand, both in the continuum [12] and on the lattice [9, 10] is the same as that of fermions due to the mapping connecting both.

However, a non-interacting treatment of the HCB expansion is invalidated by Fig. 4(a). There it is shown that at all times, even after fermionization, the density matrix decays as $1/\sqrt{x}$, a power that corresponds to HCB, and hence, the system corresponds to strongly interacting particles. Therefore, the expansion out of equilibrium leads to a new kind of bosonic state, with a Fermi edge in the momentum distribution function but still the effective one-particle states, as given by the natural orbitals, exhibit a high occupation as expected for bosons.

In what follows we study how exactly the fermionization of the momentum distribution for bosons n_k^b occurs in time, and how it depends on experimental parameters like number of particles and characteristic densities. For that we analyze the relative area between n_k^b and the momentum distribution for fermions n_k^f , $\delta = (\sum_k |n_k^b - n_k^f|) / (\sum_k n_k^b)$. This is shown in Fig. 5(a) for $\bar{\rho} = 0.51$ and different fillings of the trap. Fig. 5(a) shows that changes in n_k^b occur fast in terms of the characteristic time of the system, which is given by \hbar/t . In addition, if one chooses a criterion like $\delta = 0.05$ to state that n_k^b has fermionized, it is possible to see in the inset of Fig. 5(a) that for a given characteristic density the fermionization time (τ_F) grows linearly with the number of HCB in the trap.

Another question that is important to answer is the consequence of changing $\bar{\rho}$ in the ground state of the trap. In order to compare systems with different $\bar{\rho}$, i.e., different n_k , we display in Fig. 5(b) the ratio R between the size of the cloud once $\delta = 0.05$ and its initial size. Fig. 5(b) shows that with decreasing $\bar{\rho}$ the ratio R reduces up to ~ 2.5 , and that for $\bar{\rho} > 0.5$ it increases very fast. For low $\bar{\rho}$, such that the averaged interparticle distance is much larger than the lattice spacing, the initial lattice gas is equivalent to the one in continuous systems. This means that a fermionized n_k^b will be more easily observed in continuous systems [3] than in the lattice [2]. (In the continuous case, the asymptotic fermionization of n_k^b was obtained previously in Ref. [13].) In addition, the inset in Fig. 5(b) shows that the ratio R remains basically constant for a given characteristic density when the number of particles in the trap is changed.

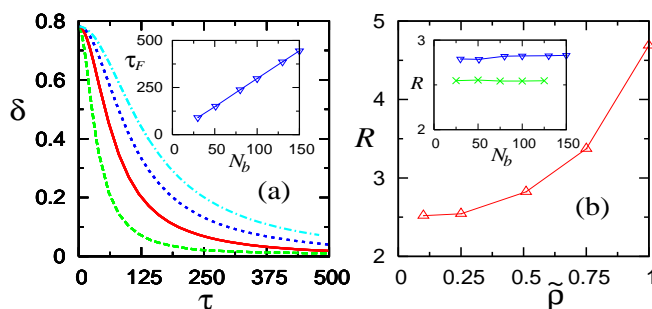


FIG. 5: (color online). Fermionization of n_k^b during the expansion of the gas. (a) Decrease of δ (see text) as a function of time for $\bar{\rho} = 0.51$; $N_b = 51$ (dashed line), $N_b = 100$ (continuous line), $N_b = 150$ (dotted line), and $N_b = 200$ (dashed-dotted line). The inset shows the fermionization time τ_F (see text) vs N_b , for $\bar{\rho} = 0.51$. (b) Ratio R between the size of gas for $\delta = 0.05$ and its original size vs $\bar{\rho}$, $N_b = 100$. The inset shows R vs N_b for $\bar{\rho} = 0.25$ (\times) and $\bar{\rho} = 0.51$ (∇).

Increasing the characteristic density of the initial system beyond the values in Fig. 5(b) one starts observing a behavior of δ which is different to the one seen in Fig. 5(a). The reason is that particles become more localized in the middle of the trap, and eventually after $\bar{\rho} \sim 2.6 - 2.7$ a Mott insulator appears in the system. This localization effect also generates an n_k^b which approaches to the one of the fermions in the initial state. [In the limit of all lattice sites with occupation one [10], $n_k^b(\tau = 0) = n_k^f$.] When such systems are released from the trap, quasi-long range correlations start to develop between initially uncorrelated particles and they lead to the formation of traveling quasi-condensates [10]. This generates an $n_k^b(\tau)$ at short times that may be more different to n_k^f than $n_k^b(\tau = 0)$, as it can be seen in Fig. 6. However, after long times one can see that a fermionization of n_k^b starts to occur as before for smaller $\bar{\rho}$. One should notice that as shown in Fig. 6, the time scales for the fermionization process for large $\bar{\rho}$ are very long, and always start affecting the low-momenta region first, so

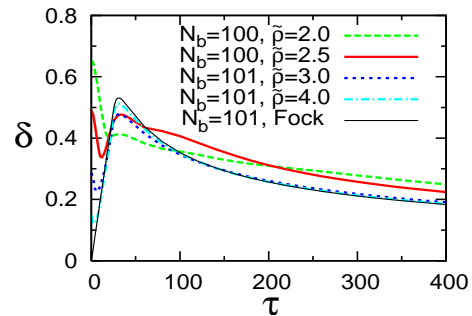


FIG. 6: (color online). Fermionization of n_k^b during the expansion of the gas. For $\bar{\rho} = 3.0$ and 4.0 a Mott insulator is formed in the middle of the trap. The behavior for a pure Fock state (Fock) with one particle per lattice site is also shown.

that still the dynamically generated quasi-condensates, which have $k \sim \pm\pi/2$, could be used as atom lasers [10].

In summary, we have shown that during the expansion of a 1D gas of HCB the momentum distribution function becomes equal to the one of the equivalent noninteracting fermions. This is an effect that can be seen experimentally in systems with [2] and without [3] an optical lattice along the 1D axes. On the other hand quantities like the NO and the OPDM still display the known behavior in equilibrium systems. In this way starting from a strongly interacting 1D Bose gas one can realize a very unconventional system of bosons displaying a Fermi edge on its momentum distribution function.

We are grateful to P. Pedri for insightful discussions, and to M. A. Cazalilla for bringing to our attention Ref. [13]. We thank HLR-Stuttgart for allocation of computer time, and to SFB 382 for financial support.

-
- [1] M. Olshanii, Phys. Rev. Lett. **81**, 938 (1998); D. S. Petrov, G. V. Shlyapnikov, and J. T. M. Walraven, *ibid.* **85**, 3745 (2000); V. Dunjko, V. Lorent, and M. Olshanii, *ibid.* **86**, 5413 (2001).
 - [2] B. Paredes *et al.*, Nature (London) **429**, 277 (2004).
 - [3] T. Kinoshita, T. Wenger, and D. S. Weiss, Science **305**, 1125 (2004).
 - [4] M. Girardeau, J. Math. Phys. **1**, 516 (1960).
 - [5] A. Lenard, J. Math. Phys. **5**, 930 (1964); H. G. Vaidya and C. A. Tracy, Phys. Rev. Lett. **42**, 3 (1979).
 - [6] O. Penrose and L. Onsager, Phys. Rev. **104**, 576 (1956).
 - [7] M. A. Cazalilla, J. Phys. B **37**, S1 (2004).
 - [8] P. J. Forrester *et al.*, Phys. Rev. A **67**, 043607 (2003); D. M. Gangardt, J. Phys. A **37**, 9335 (2004).
 - [9] M. Rigol and A. Muramatsu, Phys. Rev. A **70**, 031603(R) (2004); *ibid.* Phys. Rev. A **72**, 013604 (2005).
 - [10] M. Rigol and A. Muramatsu, Phys. Rev. Lett. **93**, 230404 (2004).
 - [11] P. Pedri, *Dynamical behavior of ultracold atomic gases*, PhD Thesis, University of Trento, Italy, 2004.
 - [12] P. Öhberg and L. Santos, Phys. Rev. Lett. **89**, 240402 (2002); P. Pedri *et al.*, Phys. Rev. A **68**, 043601 (2003).
 - [13] B. Sutherland, Phys. Rev. Lett. **80**, 3678 (1998).